The effect of the progressive consolidation of sterile lobes around the salpinx on windborne pollination may be likened to a snow fence. Particulate matter carried by the airflow is discharged on the downwind surfaces as a result of a sharp drop in airflow rate. As the PL become reduced in length and fuse acropetally, they produce a "snow fence" around the salpinx. On the basis of the data accrued by wind tunnel analyses, the localization of the snow fence increases the probability of pollination, suggesting that high efficiency in trapping pollen was a strong selective pressure involved in the evolution of the early seed plants. The data from models of *Stamnostoma* and *Eurystoma* are consistent with the snow fence scenario. As cupule axes become reduced in length and fuse acropetally, the number of pseudopollen impacting with cupule-ovule surfaces increases.

Isolated ovules of *Eurystoma* (Fig. 1I) are more efficient in trapping pollen than are cupulate ovules (Table 1). Statistically, a greater number of direct impacts occur, and a higher percentage of these reach the salpinx. Cupules of *Stamnostoma* have much the same effect and reduce the number of pseudopollen to ovule surface impacts, but they do not statistically reduce the percentage of pseudopollen which reaches the salpinx (Table 1).

The "snow fence" scenario is, however, an oversimplification. Analyses of hirsute ovules (*Salpingostoma* and *Physostoma*) indicate that the potential benefits of streamlining are mitigated by the presence of hair-bearing surfaces. Similarly, cupule axes appear to interfere with the full hypothetical potential for pollination. These data may indicate that additional selective pressures other than pollination efficiency have dictated ovule and cupule streamlining. The aerodynamic trend of ovule streamlining may have been influenced by other selective pressures such as predation. Adduction and fusion of lobes around the nucellus, the production of surface hairs, and the consolidation of many ovules into a cupule, may have served both to protect the seed or seeds or aid in their dispersal (or both). The above analyses indicate, however, that at least one significant consequence of ovule streamlining, whether through direct or indirect selective pressure, was to increase the probability of directing windborne pollen toward the salpinx and later toward the micropyle.

KARL J. NIKLAS
Division of Biological Sciences, Cornell University, Ithaca, New York 14853

References and Notes

1. H. N. Andrews, *Science* **142**, 925 (1963); A. G. Long, *Trans. R. Soc. Edinburgh* **66**, 345 (1966).
2. K. J. Niklas, B. H. Tiffney, A. H. Knoll, in *Evolutionary Biology*, M. K. Hecht, W. C. Steere, B. Wallace, Eds. (Plenum, New York, 1980), vol. 12, pp. 1–89.
3. N. E. Hughes and J. Smart, in *The Fossil Record*, W. B. Harland *et al.*, Eds. (Geological Society of London, London, 1967), pp. 107–117.
4. Flow visualization is effected by an SAI bubble generator (Sage Action, Inc., P.O. Box 416, Ithaca, N.Y. 14850) which generates neutrally buoyant helium-filled bubbles. Models are painted with a low-reflectivity paint and photographed with Tri-X Pan (ASA 400) film.
5. Airflow analogy between the model and size of ovule (Table 1) requires that the ratio of inertial and frictional forces (Reynold's number) is constant for each, such that, $Re = Vd/\nu$, Values necessary to compute Reynold's numbers are given in Table 1.
6. I thank B. Bernstein for constructing ovule and cupule models as well as illustrating flow patterns, and B. Colthart for photographic assistance. The assistance of Sage Action personnel is also gratefully acknowledged. Supported by NSF grant DEB 78-22646.

15 May 1980; revised 23 July 1980

A Scanning Micropipette Molecule Microscope

Abstract. *A movable quartz micropipette, whose tip is sealed with a polymer plug, is used as a liquid-vacuum interface to a mass spectrometer. A light microscope allows observation of, and positioning of, the micropipette tip on the surface of a sample mounted in a perfusion chamber. This forms the basis of an instrument which enables one to study, in vitro, the localization of transepithelial transport of water and other molecules. Some preliminary results from the use of this instrument are presented.*

The in vitro localization of the pathways of water transport is a problem of general interest in epithelial physiology. We have developed an instrument which provides a direct, real-time measure of water transport, with a spatial resolution of 2 to 5 μm, across a living epithelium.

A simplified diagram is shown in Fig. 1a. The instrument consists of a perfusion chamber that will allow simultaneous observation of a sample and the tip, 1 to 10 μm in diameter, of a quartz micropipette. The tip of the micropipette is sealed with a small plug of a permeable material such as dimethyl siloxane–polycarbonate copolymer or cellulose acetate (Fig. 1b) (*1*). The shank of the micropipette is connected by means of a flexible vacuum coupling to the inlet of the ionizer of a quadrupole mass spectrometer and is hence under vacuum. The micropipette is inserted in solution and scanned over (or placed at various points on) the surface of the sample, much as in the microelectrode experiments of Frömter and Diamond (*2*). Molecules that permeate the plug in sufficient amount can be detected by the quad-

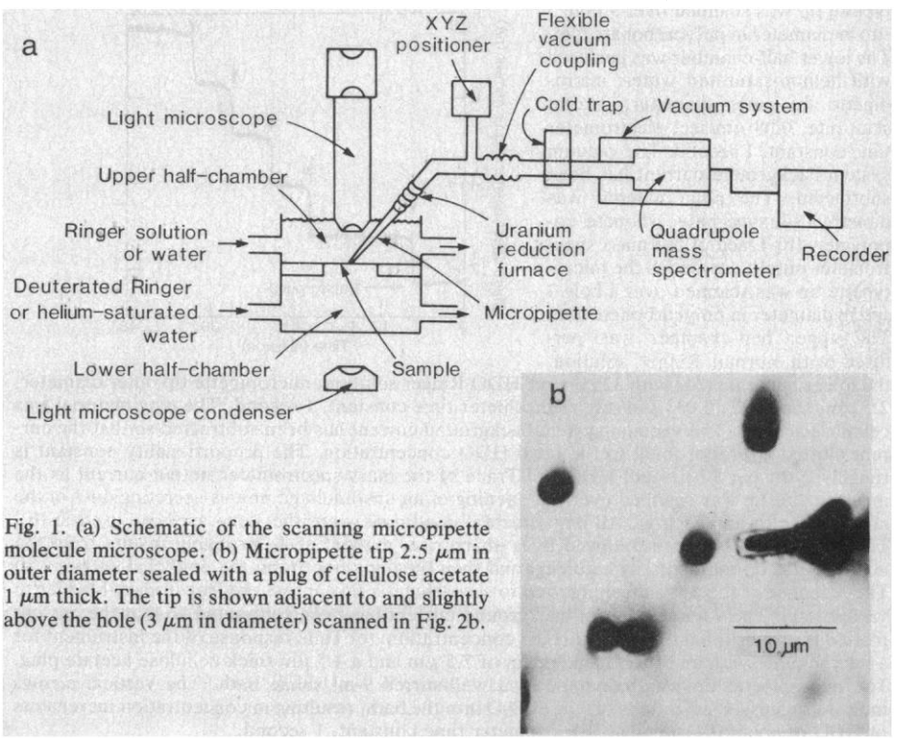

Fig. 1. (a) Schematic of the scanning micropipette molecule microscope. (b) Micropipette tip 2.5 μm in outer diameter sealed with a plug of cellulose acetate 1 μm thick. The tip is shown adjacent to and slightly above the hole (3 μm in diameter) scanned in Fig. 2b.

0036-8075/81/0116-0277$00.50/0

rupole mass spectrometer. Thus spatial variations in the concentrations of the permeating molecules can be mapped out and correlated with the in vitro morphology as observed with the light microscope.

The instrument was first used to detect spatial variations in fluxes of dissolved helium. Under these conditions we demonstrated the resolution of the apparatus by detecting the flow of helium-saturated water through holes 5 μm in diameter in a polycarbonate film (Nuclepore) 10 μm thick with a probe 3 μm in diameter (Fig. 2a).

The instrument was subsequently adapted for the detection of deuterated water fluxes by the addition of a liquid nitrogen cold trap and an in-line uranium reduction furnace based on that of Nief and Botter (*3*). The furnace consists of a thin (0.0025 cm thick) uranium foil inside the shank of the micropipette. A small heater coil wrapped around the micropipette shank and over the foil heats the foil to 650°C. At this temperature, the uranium reduces HDO to HD and UO_2 and H_2O to H_2 and UO_2 (*4*), with an efficiency close to unity. This conversion step results in good time response and sensitivity, since HD and H_2 do not adsorb significantly with the long time constants characteristic of water, and HD ionizes to produce a mass-to-charge ratio of 3, one at which little background is present in a typical vacuum system. The cold trap prevents the water background in the mass spectrometer vacuum system (0.015 percent of which is HDO) from migrating back to the uranium strip, where it would otherwise be reduced, producing a large background signal. Test pattern results for deuterated water flux across a piece of Nuclepore are shown in Fig. 2b (*5*).

Figure 2c is a scan over the opening of the duct of an unstimulated mucus-secreting gland in frog abdominal skin (*Rana pipiens*) and shows marked similarity to Fig. 2b. The maximum signal over the duct is nearly three times as large as that over the epithelium, thus indicating that the flux density of HDO emerging from the gland duct opening is significantly higher than that through the epithelial cell layers.

Figure 2d illustrates the response of frog urinary bladder (*Rana pipiens*) to vasopressin. The tissue was mounted, serosal side up with similar isotonic mucosal and serosal baths except that about 32 percent of the water in the mucosal bath was HDO rather than H_2O. The probe tip, 8 μm in diameter, was placed in contact with the serosa. Vasopressin was added and the response monitored. A substantial rapid increase, which then decayed to a more sustained but elevated level, was observed.

The theoretical sensitivity of this instrument is determined by the internal diameter of the micropipette tip, the permeability of the plug, the overall efficiency of detection of the mass spectrometer, and, for water, the conversion efficiency to hydrogen. In practice, the sensitivity is limited by signal-to-noise considerations arising from whatever background is present at the selected mass-to-charge ratio peak. The observed and predicted sensitivity are equal within the limits of experimental accuracy for dimethyl siloxane–polycarbonate plugs. For cellulose acetate plugs, the observed sensitivity is less than might be expected (*6*). Figure 2e shows the instrument time response, with a micropipette having a tip diameter of 7.5 μm, to successive increases in HDO concentration in a well-stirred bath.

Spatial resolution is governed by diffusion and is thus a function of the micropipette tip size, the degree of "stirring" in the perfusion chamber (that is, the boundary layer thickness above the sample), and the separation between the micropipette tip and the sample. On robust samples, such as Nuclepore filter or frog skin, providing sufficient flow to produce good resolution is no problem.

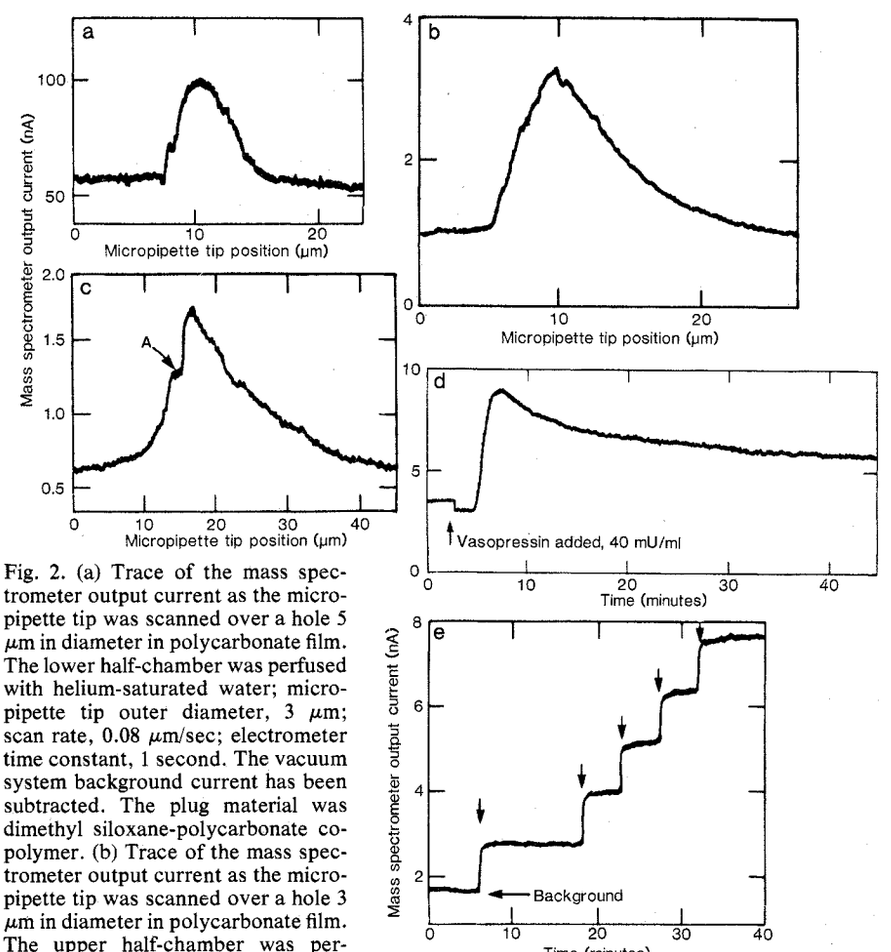

Fig. 2. (a) Trace of the mass spectrometer output current as the micropipette tip was scanned over a hole 5 μm in diameter in polycarbonate film. The lower half-chamber was perfused with helium-saturated water; micropipette tip outer diameter, 3 μm; scan rate, 0.08 μm/sec; electrometer time constant, 1 second. The vacuum system background current has been subtracted. The plug material was dimethyl siloxane-polycarbonate copolymer. (b) Trace of the mass spectrometer output current as the micropipette tip was scanned over a hole 3 μm in diameter in polycarbonate film. The upper half-chamber was perfused with normal Ringer solution, the lower half-chamber with 32 percent HDO Ringer solution; micropipette tip outer diameter, 2.5 μm; scan rate, 0.033 μm/sec; electrometer time constant, 1 second. The plug material was cellulose acetate. The vacuum system background current has been subtracted so that the current plotted is proportional to the local HDO concentration. The proportionality constant is roughly 2 nA per 10 percent HDO. (c) Trace of the mass spectrometer output current as the micropipette tip was scanned over the opening of an unstimulated mucus-secreting duct in the abdominal skin of the frog. All experimental conditions were the same as those used in (b). The period of no change followed by a sharp rise, marked at *A*, probably results from the micropipette tip momentarily catching, and then breaking free from, the epithelial surface. (d) The response of the diffusional mucosal to serosal water flux across the frog urinary bladder to vasopressin. The vacuum system background current has been subtracted so that the current plotted is proportional to the local HDO concentration. (e) Time response of the instrument for a micropipette with an outer diameter tip of 7.5 μm and a 4.5 μm-thick cellulose acetate plug. The micropipette tip was immersed in a well-stirred 9-ml saline bath. The vertical arrows indicate successive injections of 5 μl of D_2O into the bath, resulting in concentration increments of HDO of about 0.11 percent. Electrometer time constant, 1 second.

On more fragile samples, such as frog or toad urinary bladder, where we have been examining the relative permeabilities of the granular and mitochondria-rich cells before and after stimulation by vasopressin, the required flow rates generate shear forces that cause the tissue to degenerate rapidly. This problem can be eliminated if a second micropipette (tip diameter, approximately 5 to 10 μm) is introduced to provide substantial flow only in the immediate vicinity of the sampling micropipette tip.

The results presented here reflect a few of the possible applications of scanning micropipette molecule microscopy to problems in biology and medicine. Even in a nonscanning mode, the rapid time response and small volume sampled could be used to great advantage in studies of preparations such as isolated tubules or capillaries. Furthermore, for many applications, a high-grade mass spectrometer is not necessary, since the conversion of HDO to HD reduces the necessary resolving capability of the mass spectrometer substantially. A modified leak detector might suffice for many applications.

JOSEPH A. JARRELL
Research Laboratory of Electronics and *Department of Physics, Massachusetts Institute of Technology, Cambridge 02139,* and *Laboratory of Renal Biophysics, Medical Services, Massachusetts General Hospital, Boston 02114*
JOHN G. KING
Research Laboratory of Electronics and *Department of Physics, Massachusetts Institute of Technology*
JOHN W. MILLS
Laboratory of Renal Biophysics, Medical Services, Massachusetts General Hospital, and *Department of Anatomy, Harvard Medical School, Boston, Massachusetts 02115*

References and Notes

1. The micropipettes are plugged by being dipped into a solution of the plug material in a volatile solvent. Internal overpressure is used to oppose capillarity and thus to regulate the length of the slug of solution drawn into the tip and hence the thickness of the polymer plug that remains after the solvent evaporates. Further details of micropipette construction and the rest of the instrument are given in J. A. Jarrell and J. G. King, in preparation.
2. E. Frömter and J. Diamond, *Nature (London) New Biol.* **235**, 9 (1972).
3. G. Nief and R. Botter, *Advances in Mass Spectrometry* (Pergamon, Oxford, 1959), pp. 515–525.
4. D. Halliday and A. Miller, *Biomed. Mass Spectrom.* 4, 82 (1977).
5. The peak in Fig. 2b is wider than that in Fig. 2a. This is most likely the result of greater diffusional broadening since both the pressure head (about 10 cm of water) and hole diameter used to generate Fig. 2b were smaller than those used for Fig. 2a, resulting in a lower emergent fluid velocity. Many other factors may be involved, however. The low solubility of helium in water relative to the high "solubility" of water in water causes the micropipette plug to act as a "low-impedance" probe for dissolved helium in which depletion of the surrounding solution is significant. For water the micropipette acts as a "high-impedance" probe. Moreover, the microcirculation of the unlabeled water in the upper half-chamber can affect the concentration profile of emerging labeled water.
6. Cellulose acetate plugs, although approximately 20 to 100 times more permeable than dimethyl siloxane-polycarbonate plugs, are less permeable by at least a factor of 10 than might be expected on the basis of literature values. A possible explanation is that the permeability of cellulose acetate is known to be a function of its degree of hydration. Clearly, the vacuum side of the plug is not fully hydrated. Also, there seems to be some variability of cellulose acetate permeability from plug to plug. This is not easy to quantify in view of the limited accuracy to which plug dimensions can be measured.
7. Supported by Johnson & Johnson Associated Industries Fund, Whitaker Health Science Fund, Francis L. Friedman Chair, NIH grant HL-06664, and a Hoechst-Roussel/National Kidney Foundation fellowship. We acknowledge discussions with D. DiBona, A. Essig, M. Lang, A. Leaf, S. Rosenthal, and J. Weaver.

28 July 1980

Diatoms as Hydrographic Tracers: Example from Bering Sea Sediments

Abstract. *Variations in the distribution of diatom species in surface sediments mirror distinct hydrographic regimes on the Bering shelf. Spring salinity fronts divide the water column into four zones with different vertical structures and different productivity patterns. Four assemblages of diatoms can be distinguished in sediments underlying the zones.*

The PROBES (Processes and Resources of the Bering Sea) project is a multidisciplinary study designed to investigate the relations between hydrography, productivity, and food-web structure in the southeast Bering Sea. Fieldwork over several years (*1*) has determined the basic hydrography and productivity of the area. The work has included hydrographic and nutrient measurements, analyses of plankton and chlorophyll, and counts of birds and fish.

In May 1979, during Leg 2 of the PROBES study, a series of bottom-grab samples were taken along the station track line (Fig. 1A). I examined the nu-

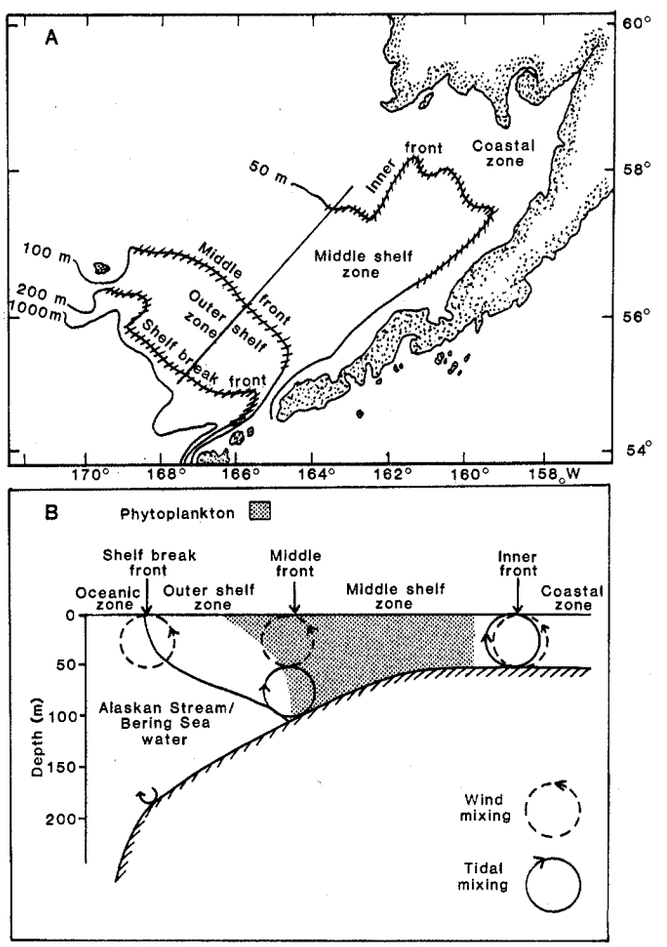

Fig. 1. Map of the region of the Bering shelf studied by PROBES, showing interpreted fronts and zones (*1*). (A) Horizontal distribution of the fronts. The straight line indicates the transect of Leg 2. (B) Schematic diagram of vertical structure and productivity in the area.

0036-8075/81/0116-0279$00.50/0